An Approximate Method to Solve Two-Dimensional Laplace's Equation by Means of Superposition of Green's Functions on a Riemann Surface

SADAYUKI MURASHIMA* and HIDEO KUHARA**

A new method of solving two dimensional Laplace equation is presented. This method is a superposition method of Green's function on a Riemann surface constructed by a complex transformation and is suitable for analyzing potential problems in aregion that contains curved arcs as its boundary. This method originates from the research of the charge simulation method used often in some part of electrical engineering as an effective and simple method of solving Laplace equation. The essential and evident defect of this method is that the error of the analysis becomes large for the exterior problem of a very thin region or a region without thickness due to the singularity of Green's function superposed in this method.

To overcome this difficulty, in this paper, Rimann surface constructed by two-valued complex transformation $z=\frac{1}{2}(t+\frac{1}{t})$ is used. The poles of Green's functions are placed on one of two sheets of the Riemann surface and their influence on the other sheet is superposed similarly to the ordinary charge simulation method. By using this complex transformation, the curved arc without area is transformed into a closed region with wide area. Then we can keep the poles of Green's functions apart from the boundary. This fact enables us to reduce the influence of the singularity of Green's function.

Above technique is verified by analyzing the test problems in electrostatics. The results are fully satisfactory. This method is applicable to the problems in a region that contains many curved arcs of arbitrary shape. Hence it will be widely used for various problems in electrostatics or hydrodynamics.

1. Introduction

Laplace's equation is a typical and basic partial differential equation in theoretical physics and has been studied by many scientists and mathematicians for hundreds of years. Abundant results obtained from the studies of this equation have stimulated many researchers in various fields of science and technology. Thus far many approaches have been investigated. For example the theory of special functions has been used for hundreds of years[1,2] and much knowledge has been accumulated, but its applicability to problems in modern science and technology is too narrow; the discrete method, such as the finite element method,[3] is applicable to almost all problems (problems in a region of arbitrary shape, non-linear problems, and non-homogeneous problems), but is not necessarily effective under some conditions; the Monte Carlo method,[4] which completely depends on the function of a computer, is efficient only for some special problems, and so on.

None of these methods, or other methods presented thus far, can be applied to diverse problems in modern science and technology.

In the two-dimensional boundary value problem of the Laplace equation, the difficulty of the problem in the region that contains a curved arc as its boundary is well known. If the shape of the curve is arbitrary, no known method has been appropriate.

This paper proposes an approximate method for solving the boundary value problem in a region that contains curved arcs as its boundary. This method originates from the research of the charge simulation method,[5,6] which has been used for about 10 years in some parts of electrical engineering and is recognized as an effective and simple method of solving Laplace's equation. The charge simulation method (we will call this CSM hereafter) is a superposition method of Green's functions in the unbounded region of Laplace's equation. It corresponds to the boundary method and the collocation method[7,8] in terms of the method of weighted residuals.

In 1969, H. Steinbigler[5] first used CSM in his dissertation to compute the electrical field around a high-voltage apparatus. In the 1970s, several reports[9-15,25] related to the application of CSM were published especially in Japan and West Germany.

The CSM is not considered to be straightforward, because contour points and charge points must be determined by trial and error. However, the estimation of error in the CSM is very simple, because only the error on the boundary need be examined, since it is here the maximum error appears. A high degree of accuracy can easily be obtained if the shape of the boundary concerned is not too complicated.

*Department of Electronics, Faculty of Engineering, Kagoshima University.
**Department of Information and Electronic Engineering, Yatsushiro National College of Technology.

Its evident and essential defect[9] is that the error of the analysis becomes great for the exterior problem of a very thin region, or for a region without thickness, because of the singularity of Green's functions superposed in the CSM. Usually the charge points are placed adequately apart from the boundary to reduce the influence of the singularity of charges. For a very thin region, we must place the charges near the boundary, and hence a considerable error is inevitable. The CSM has not been considered applicable for the exterior problem of a very thin region or for a region without thickness.

To overcome this difficulty, we propose to use Green's function on a Riemann surface constructed by the two-valued complex transformation, $z=1/2(t+1/t)$. To be specific, we regard one of the two sheets of the Riemann surface as an ordinary plane on which the boundary value problem exists, and let the branch cut of the Riemann surface coincide with the curved arc (boundary) under consideration. Charges (poles of Green's function) are placed on the other sheet of the Riemann surface, and their influence on the first sheet is superposed similarly to the ordinary CSM. By this complex transformation, the curved arc (boundary) is converted to a closed curve that has a wide area within it. Then we can keep the poles of Green's function apart from the boundary. This enables us to reduce the influence of the singularity of Green's function.

Chapter 2 is a general introduction to the CSM. It discusses the error estimation and how to determine the data necessary in the CSM. In Chapter 3, we explain the structure of the Riemann surface and show graphically the behavior of Green's function on it. How to superpose Green's function in a practical problem is also shown. Chapter 4 points out several problems associated with this technique and describes their solutions. In Chapter 5, in order to verify our technique, we analyze the problems of parallel-plate condensers and curved parallel-plate condensers, well known in electrostatics. The accuracy reached in these analyses is remarkable.

In Chapter 6, we evaluate our technique and describe its application to other fields. In this paper, technical terms from Electrical Engineering are often used. Readers not familier with Electrical Engineering, may substitute those terms with the following:

Potential function due to unit charge: Green's function
Charge points: Poles of Green's function
Charge quantity: Weighted factor multiplied by Green's function
Conductor of Electrode: Boundary
Charge: Pole of Green's function (the latter is not a complate synonym of the former).

2. Charge Simulation Method

2.1 Principle of Charge Simulation Method

Here we consider the Dirichlet problem of Laplace's equation in a domain D, which is shown in Fig. 1. For simplicity, we consider a problem in two dimensions:

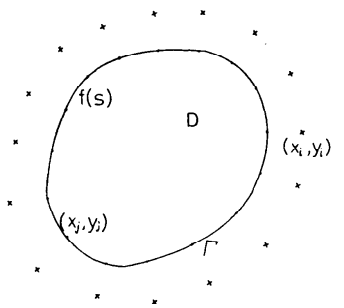

Fig. 1 Arrangement of charges and contour points for the calculation of the potential Dirichlet-type problem.

$$\nabla^2\psi(x, y)=0, \quad (x, y) \in \boldsymbol{D}, \tag{1}$$

$$\psi(x, y)_\Gamma=f(s), \quad (x, y) \in \boldsymbol{\Gamma}, \tag{2}$$

where Γ is the boundary, and $f(s)$ is the boundary value at any boundary point, s. In the CSM, the general solution $\phi(x, y)$ of the preceding Laplace equation is expressed by means of superposition of potential function due to several charges at charge point (x_i, y_i) external to D. That is,

$$\phi(x, y)=\sum_{i=1}^{N} Q_i \boldsymbol{G}(x, y; x_i, y_i), \tag{3}$$

where N is the number of charges, Q_i is an unknown constant, called the weighted factor or the magnitude of i-th charge, and $\boldsymbol{G}(x, y; x_i, y_i)$ is Green's function in the unbounded region due to unit line charge at (x_i, y_i). In two-dimensional problem, the function $\boldsymbol{G}(x, y; x_i, y_i)$ is as follows:

$$\boldsymbol{G}(x, y; x_i, y_i)=\frac{1}{2\pi}\log\sqrt{(x-x_i)^2+(y-y_i)^2}. \tag{4}$$

The expression (4) is a harmonic in the domain $\boldsymbol{D}$, because the charge points (x_i, y_i) are not inside the $\boldsymbol{D}$. Hence, the general solution (3) satisfies eq. (1).

To determine the solution, we impose on eq. (3), the boundary condition at suitably chosen contour points (x_j, y_j) of the same number as that of the charge points. Then,

$$\phi(x_j, y_j)=\sum_{i=1}^{N} Q_i \boldsymbol{G}(x_j, y_j; x_i, y_i)=f(s_j), \quad \text{for } j=1, 2, 3, \cdots, N \tag{5}$$

where (x_j, y_j) is the j-th contour point, and s_j also denotes the contour point. We here assume that $(x_j, y_j) \neq (x_i, y_i)$.

Solving this system of N in linear eq. (5), we can determine the N charges Q_i. Substituting Q_is into eq. (3), we get an approximate solution of the CSM. Of course, whether or not the calculated set of charges fits the boundary conditions must be checked.

2.2 The Properties of the Error in CSM[16]

Here we define the error $e(x, y)$ as the difference between calculated potential $\phi(x, y)$ and the exact potential $\psi(x, y)$, as follows:

$$e(x, y)=\psi(x, y)-\phi(x, y). \tag{6}$$

Since $\psi(x, y)$ satisfies eq. (1) and (2), and $\phi(x, y)$ satisfies eq. (1), we get:

$$\nabla^2 e(x, y)=0, \quad (x, y) \in \boldsymbol{D}, \tag{7}$$

$$e(x, y)=f(s)-\phi(x, y)_{\Gamma}, \quad (x, y) \in \Gamma. \tag{8}$$

The second term of the right side of eq. (8) is already known. Hence, the error $e(x, y)$ is the solution of the first kind of boundary value problem, with boundary value $f(s)-\phi(x, y)_{\Gamma}$. In other words, the error has the same properties as the potential. In CSM, if we examine the error on the boundary, we can determine the maximum error of solution.[17] We need not examine the error inside the domain.

In Fig. 2, we show a error distribution of the solution of the axisymmetric problem of calculating the electrical potential between a sphere $r^2+(z-3)^2=1$, which is charged to a prescribed potential $+1$, and an earthed plane at $z=0$. In the figure, the contour lines 8 and -9 denote $+10^{-8}$ and -10^{-9}, respectively. Even though the number of charges is only 7, very high accuracy is obtained. We can see that the error decreases logarithmically as the point moves away from the boundary.

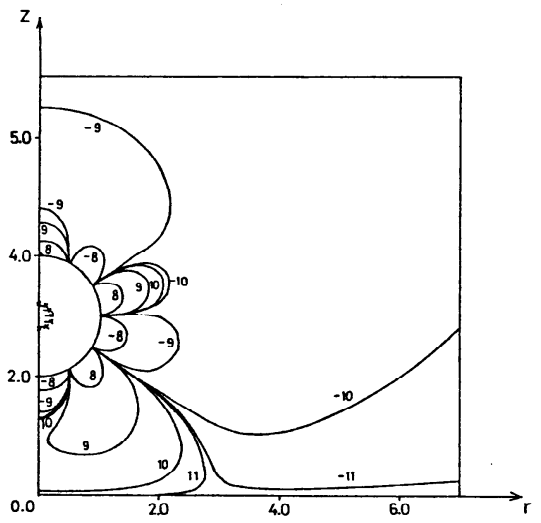

Fig. 2 Typical error distribution for the sphere-plane boundary (electrode).

2.3 How to Determine the Charge Points and Contour Points

The accuracy of CSM analysis depends, sensitively, on the charge points and contour points. How to determine the charge points and contour points is an important problem but, because of the complexity of combining them, it has not been studied. The authors present a practical and simple answer to this problem.

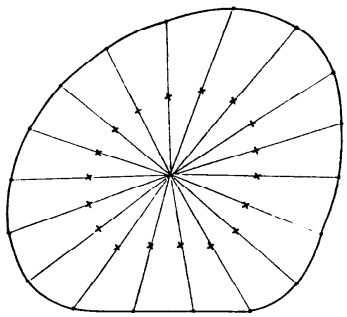

Fig. 3 Typical arrangement of contour points and charge points for a smooth closed boundary.

For the problem of the exterior field with a smoothed boundary, shown in Fig. 3 we first put contour points on the boundary so that the distances between them are nearly equal. Then we contract the boundary by the contraction ratio $R(<1)$, the center of contraction being suitably taken. We define these new points as charge points into which the contour points are converted. This means that the charges approach the boundary when R tends to 1, and they move far from the boundary as R decreases. For the interior problem, we must place them outside the boundary. By magnifying the boundary with the magnification ratio $E(>1)$, the contour points move out of the region. We define those points as charge points. If we adopt an inverse parameter $R=1/E$, we get a parameter of the same form as in the interior problem.

3. Charge Simulation Method Using Riemann Surface

3.1 Application of Conformal Transformation

Eq. (4), superposed in the CSM, is equal to the real part of Green's complex function in an unbounded region

$$G(z; z_i)=\frac{1}{2\pi}\log(z-z_i), \tag{9}$$

where $z=x+iy$ and $z_i=x_i+iy_i$. Equation (4) is harmonic and satisfies Laplace equation, except for $z=z_i$ and $z=\infty$. An application of a conformal transformation to a harmonic function has no influence on the property of the harmonic function. Various conformal transformations produce many test function available for various objects in the CSM. For example, one of the authors used Green's function in a bounded region determined by a conformal transformation in order to reduce the number of charges and, consequently, the computing time.[18]

The underlying context in this paper is that although we transform the unbounded region into the Riemann surface with two sheets, we use Green's function on

each sheet of the Riemann surface.[19] Green's function on the Riemann surface is also harmonic; i.e., it is the solution of Laplace's equation.

3.2 Properties of Conformal Transformation $z=1/2(t+1/t)$

The conformal transformation, $z=1/2(t+1/t)$, quite often appears in numerical analysis.[20] By simple reduction, we obtain the inverse transformation as follows:

$$t=z+\sqrt{z^2-1}, \tag{10}$$

$$t=z-\sqrt{z^2-1}, \tag{11}$$

where $\sqrt{z^2-1}$ is a complex function that takes the value $\sqrt{3}$ at $z=2$. By these two transformation equations, the curved line that connects two points $(-1, 0)$ and $(1, 0)$ is transformed into a closed line on the t-plane. In Fig. 4, some curved arcs on the t-plane and corresponding closed lines are shown. One of the two sheets is mapped to the outer region of the closed line by eq. (10), and the other sheet is mapped to the inner region by eq. (11). Because the branch cut of the Riemann surface attached to the mapping $\sqrt{z^2-1}$ is allowed to be arbitrary in shape, we select its shape in z-plane so as to coincide with the curved arc on which the boundary value of the problem is assigned. The closed curve in t-plane, which is the image of this branch cut, is divided into the upper part, and lower part, corresponding to the curved arc being considered as in the sheet 1, and sheet 2, of the Riemann surface with the prescribed branch cut, respectively.

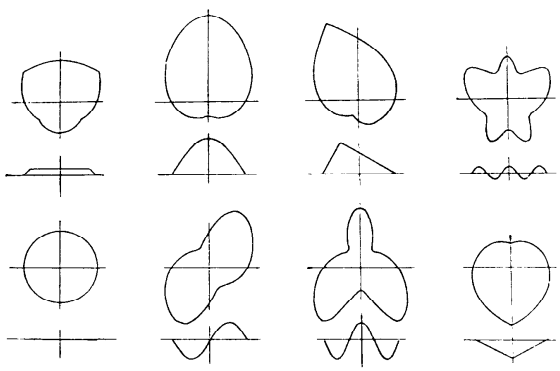

Fig. 4 Transformation of a curved cut to a closed line by $z=1/2(t+1/t)$.

3.3 Green's Function on Riemann Surface

Green's complex function on an unbounded t-plane is

$$G(t; t_i)=\frac{1}{2\pi}\log(t-t_i),$$

where t_i is the pole of Green's function. Substituting t and t_i expressed by eqs. (10) and (11) into this equation, we get

$$G(z; z_i)=\frac{1}{2\pi}\times\begin{cases}\log(z+\sqrt{z^2-1}-z_i-\sqrt{z_i^2-1}), & z, z_i\in S.1 \quad \text{(a)}\\ \log(z-\sqrt{z^2-1}-z_i-\sqrt{z_i^2-1}), & z\in S.2, z_i\in S.1 \quad \text{(b)}\\ \log(z+\sqrt{z^2-1}-z_i+\sqrt{z_i^2-1}), & z\in S.1, z_i\in S.2 \quad \text{(c)}\\ \log(z-\sqrt{z^2-1}-z_i+\sqrt{z_i^2-1}), & z, z_i\in S.2 \quad \text{(d)}\end{cases} \tag{12}$$

where the expressions in (a) and (b) are the representations of Green's function on sheet 1 and sheet 2, respectively, and correspond to the pole of Green's function on sheet 1. Eqs. (c) and (d) are similar representations corresponding to the pole of Green's function on sheet 2.

In Fig. 5, the contour lines of the real and imaginary parts of Green's complex function (12) are shown. In Fig. 5, the graphs (a), (b), (c) and (d) correspond to the expressions (a), (b), (c) and (d) of eq. (12), respectively. The shape of the branch cut in Fig. 5 is a straight line between $(-1, 0)$ and $(1, 0)$. The discontinuity in value of the real and imaginary parts is seen on the straight branch cut. However, if we inspect the graphs, overlapping Fig. 5(a) on Fig. 5(b), we can see that the contour lines in the former continue smoothly to that in the latter by crossing the branch cut. For the pair of Fig. 5(c) and (d), the same is true. The complex logarithmic function is a multivalued function. Hence, the argument is arbitrary by $2\pi n$, where n is an integer. Here restrict $(1/2\pi)\arg(z)$ to between $-1/2$ and $1/2$. The discontinuity line of the imaginary part at $Im(G)=\pm 0.5$ goes on artificially. This is because the graphic program is incomplete, partly because of the lack of time and partly because of the programming technique. Actually, the discontinuity line goes on smoothly.

The value of Green's function on each sheet depends on the shape of the branch cut. In Fig. 6, Green's function for a non-straight cut is shown. Graphs (a), (b), (c) and (d) in Fig. 6 are equal to those in the previous figure, except for the shape of the branch cut.

Since our idea is that to solve the boundary value problem on sheet 1, we must locate the poles of Green's function on sheet 2 and use its influence on sheet 1, then eq. (c) among the 4 equations in (12) is important

$$G(z; z_i)=\frac{1}{2\pi}\log(z+\sqrt{z^2-1}-z_i+\sqrt{z_i^2-1}). \tag{13}$$

Three other eqs. (a), (b) and (d) also can be used in the CSM, because they are all harmonic. However, it is not yet obvious whether or not they are useful.

The complex representation of Green's function is given here, because it simplifies the theory and enables us to make concise programs. In reality, we use the real part of the Green's complex function; i.e.,

$$g(x, y; x_i, y_i)=R_e\{G(z; z_i)\}, \tag{14}$$

where $R_e\{A\}$ denotes the real part of A. Moreover, the gradients of function g in either x or y direction are given

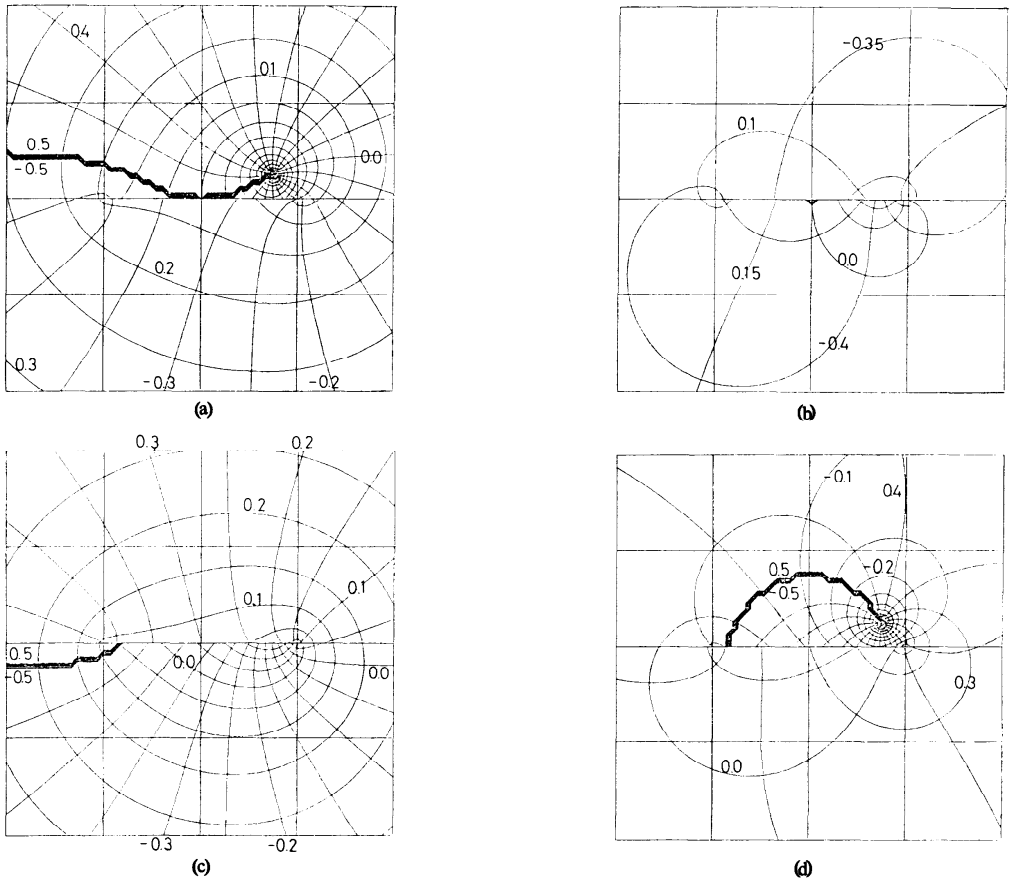

Fig. 5 Green's functions on Riemann surface with a straight cut and a source at (0.75, 0.25).

by:

$$\frac{\partial g}{\partial x}=R_e\left\{\frac{\partial G}{\partial z}\right\}, \tag{15}$$

$$\frac{\partial g}{\partial y}=-I_m\left\{\frac{\partial G}{\partial z}\right\}, \tag{16}$$

where

$$\frac{\partial G}{\partial z}=\frac{1}{2\pi}\frac{1+\dfrac{z}{\sqrt{z^2-1}}}{z+\sqrt{z^2-1}-z_i+\sqrt{z_i^2-1}} \tag{17}$$

3.4 The Application to Practical Problems Containing Many Curved Arcs

Here we consider the Dirichlet problem of Laplace's equation in domain D, which contains two curved arcs as its boundary, as shown in Fig. 7(a). The prescribed boundary value on the outer boundary is V_0, and the values on the two inner boundaries are V_1 and V_2, respectively. Charges are represented in Fig. 7 by three kinds of notations: ×, △ and ○. Their meanings are

×: Green's function on the ordinary plane,

△: Green's function on the Riemann surface with two branch points, A and B, and

○: Green's function on the Riemann surface with two branch points, C and D.

The numbers of these three kinds of Green's function are N_0, N_1 and N_2, respectively. The shape of the branch cut of the above two Riemann surfaces must, of course, coincide with those of corresponding curved arcs.

The poles of the three kinds of Green's function are located around the corresponding curved arcs, as shown in Fig. 7(a). These expressions, in formulae, are:

$$\phi(x, y)=\sum_{i=1}^{N} Q_i R_e\{G(z; z_i)\}, \tag{18}$$

where $N=N_0+N_1+N_2$

and

$$G(z; z_i)=\frac{1}{2\pi} \times \begin{cases} \log(z-z_i), & 0<i\leqq N_0 \\ \log\{z+\sqrt{(z-A)(z-B)}-z_i+\sqrt{(z_i-A)(z_i-B)}\}, & N_0+1\leqq i\leqq N_0+N_1 \\ \log\{z+\sqrt{(z-C)(z-D)}-z_i+\sqrt{(z_i-C)(z_i-D)}\}, & N_0+N_1+1\leqq i\leqq N. \end{cases} \tag{19}$$

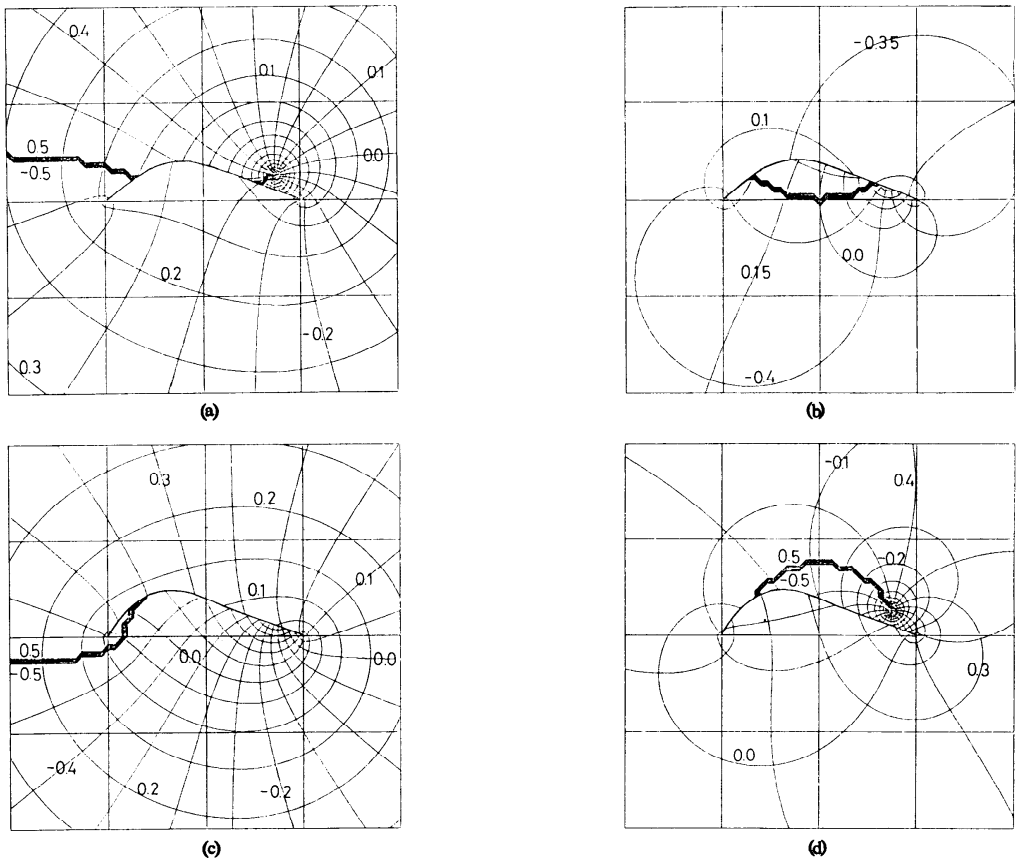

Fig. 6 Green's functions on Riemann surface with a curved cut and a source at (0.75, 0.25).

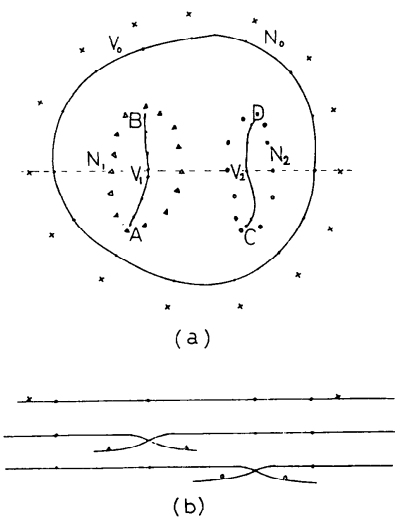

Fig. 7 How to use Green's functions for a practical problem.

The cross sections of the Riemann surface are depicted in Fig. 7(b). Charges denoted by × are on the ordinary plane, and charges denoted by △, and ○, are on sheet 2 of the Riemann surface having the curved arc AB, and CD, as its branch cut, respectively. It is obvious that this technique is applicable to the problem in a region that has many curved arcs. We also can apply this method without difficulty to thick, but very narrow regions, and to wide, but partially thin regions.

4. The Problems of Numerical Computation

The contents in the previous chapter are insufficient to practical computation of our problem. Several problems must be solved to implement our technique.

4.1 Computation of Complex Function $\sqrt{z^2-1}$

The complex function $\sqrt{z^2-1}$, with a branch cut of arbitrary shape, is necessary to map the z-plane on the t-plane. The complex function $\sqrt{z^2-1}$ must be continuous in the region except on the branch cut, which runs from $(-1, 0)$ to $(1, 0)$. Using the standard square root function, CSQRT(Z), which is built into the computer, the result of CSQRT($Z^*Z-1.0$) applied to $\sqrt{z^2-1}$ has values of oposite sign in some parts. In order to make

the function that we need, we must use the following sign manipulation*.

4.1.1 Straight Cut

$$\sqrt{z^2-1}=\begin{cases}\text{CSQRT}\,(z^*z-1.0), & (x,y)\in E_1,\\ -\text{CSQRT}\,(z^*z-1.0), & (x,y)\in \bar{E}_1,\end{cases} \tag{20}$$

where $z=x+iy$, E_1 is the sum of three areas ($x\geqq 0$, $y\geqq 0$), ($x>0, y<0$) and ($y=0, -1\leqq x<0$), shown in Fig. 8, and $\bar{E}_1$ is the complement of E_1. Equation (20) is discontinuous on the straight branch cut, and the value of the function on the cut is equal to the limiting value when we approach the cut from the upper side.

4.1.2 Non-straight cut

The shape of the branch cut is curved and assumed to be $y=F(x)>0$ for $-1\leqq x\leqq 1$ and $F(\pm 1)=0$, as shown in Fig. 9. Then:

$$\sqrt{z^2-1}=\begin{cases}\text{CSQRT}\,(z^*z-1.0), & (x,y)\in E_2,\\ -\text{CSQRT}\,(z^*z-1.0), & (x,y)\in E_2,\end{cases} \tag{21}$$

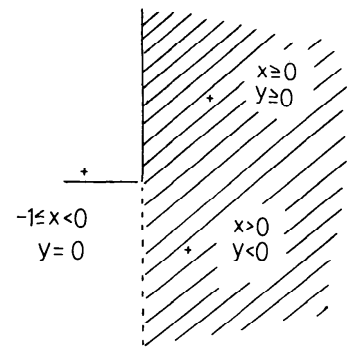

Fig. 8 Area E_1 used for the computation of $\sqrt{z^2-1}$ with a straight cut.

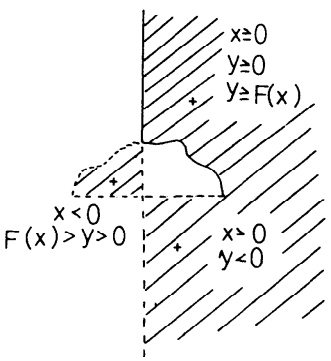

Fig. 9 Area E_2 used for the computation of $\sqrt{z^2-1}$ with a curved cut.

*The resulting sign of computation is not always common in all computers, but the Fortran system on the Facom 230-45s of Kagoshima University, and the HITAC 8800 at the computer center of Tokyo University, well perform this procedure.

where the area E_2 is the sum of three areas ($x\geqq 0, y\geqq 0$, $y\geqq F(x)$), ($x>0, y<0$) and ($x<0, F(x)>y>0$). Equation (21) is discontinuous on the curved cut, and the value on the cut is considered to be continuous when we reach the cut from the upper side, as in the previous case.

4.1.3 More complicated cut

If the branch cut runs from $(-1, 0)$ to $(1, 0)$ with twist and turn as shown in Fig. 10(a), sign manipulation becomes more complicated. In the areas marked with a + sign among the several areas divided by the imaginary axis, the straight line between $(-1, 0)$ and $(1, 0)$ and the curved branch cut, we adopt $+\text{CSQRT}(Z^*Z-1.0)$ and the expression of opposite sign in the other areas. In Fig. 10(b), the bold line means belonging to the + area; the dotted boundary does not belong to the + area.

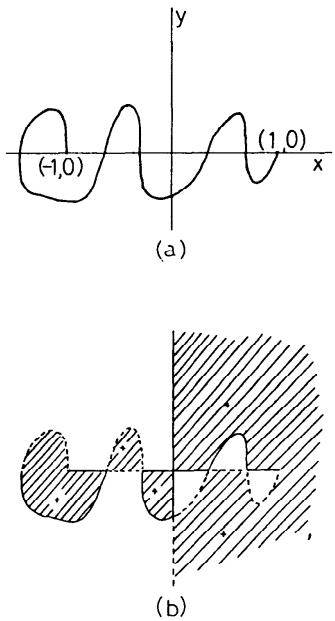

Fig. 10 The case of more complicated cut.

4.2 Which Sheet does the Branch Cut Belong to?

The branch cut connects two sheets. To which sheet, 1 or 2, does the branch cut belong? It belongs to both sheets. In other words, it is a combination of the cuts belonging to sheets 1 and 2. When the transformation to the t-plane is executed, the cut on sheet 1 is mapped to the upper part of the closed line in the t-plane, and the cut on sheet 2 is mapped to the lower part. Thus, the closed line is completed, and the single valuedness of $z=1/2(t+1/t)$ is assured.

Hence, one must provide additional data to decide to which sheet the contour points or the charge points belong. This is one factor of our method that differs from the ordinary CSM. Since the boundary value problem we are considering exists on sheet 1, we must compute

the potential by specifying index 1. There are two cases of index 1 and 2 for the potential on the curved arc. In each case, the potential is equal to the limiting value that is given when one approaches the curved arc from both the upper and lower sides, or, in other words, the potential on the curved arc has two values.

The use of this index on the curved arc becomes complicated for the problem that has many curved arcs. On the index of the potential point on one of many curved arcs, index 2 is effective only when the potential point is on the branch cut of the Riemann surface on which the charge concerned exists. If the potential point and the charge are on different Riemann surfaces, there is no distinction between indexes 1 and 2; then index 1 should always be used (see Fig. 7(b)).

5. Numerical Examples

5.1 Parallel Plate Condenser

In Fig. 11, an infinitely long parallel plate condenser with a width of 2 (in arbitrary units) is arranged with a distance of $2D$ between the plates. The potentials of the upper and lower electrodes are assigned $+1$ and -1, respectively. The contour points are designated in the t-plane by dividing the unit circle in to N-equal parts. When this unit circle contracts by the ratio R, we designate the positions at which the contour points correspond as charge points. Since, in practical computation, data (contour points, charge points, and check points) is given by the value in the z-plane, then all of the above data should be given by values in the z-plane. Hence, contour points have the value on the straight line that connects points $(-1, D)$ and $(1, D)$, and charge points are arranged on the elliptic circle, with foci of $(-1, D)$ and $(1, D)$. The contour points need additional data denoting to which sheet each contour point belongs. The charge points do not need such data, because they are all on sheet 2.

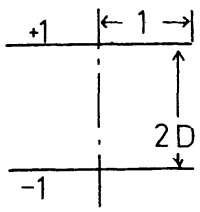

Fig. 11 Parallel plate condenser in two dimensions.

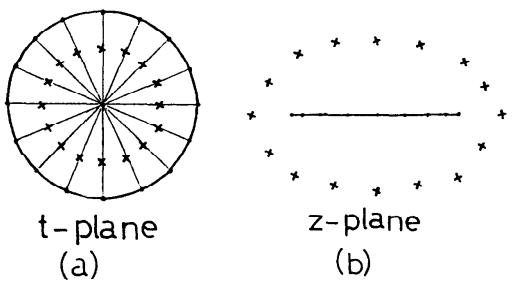

Fig. 12 Arrangement of contour points and charge points for the parallel plate condenser.

As R tends to 1, charge points approach the boundary, and as R tends to 0, charges move far away from the boundary and, consequently, the charge points are distributed in a circle of a large radius. The contour points in the z-plane distribute densely near the tips of the plate, and sparsely near both sides of the center of the plate (see Fig. 12(b)).

We halved the number of unknown constants, using symmetry of the upper and lower electrodes. We did not, however, use the symmetry of right and left, because the program was designed to treat non-symmetric problems. Fig. 13 shows typical error distribution on the boundary (electrode). The error vanishes at the contour points and oscillates to a + or − direction between the contour points. Estimation of the error F is the mean square root of errors on the boundary. By locating several checkpoints (here we locate 3 checkpoints; one checkpoint may be enough) between contour points, we estimate the error as follows:

$$F=\sqrt{\sum_{i=1}^{M} E_i^2/M}, \tag{22}$$

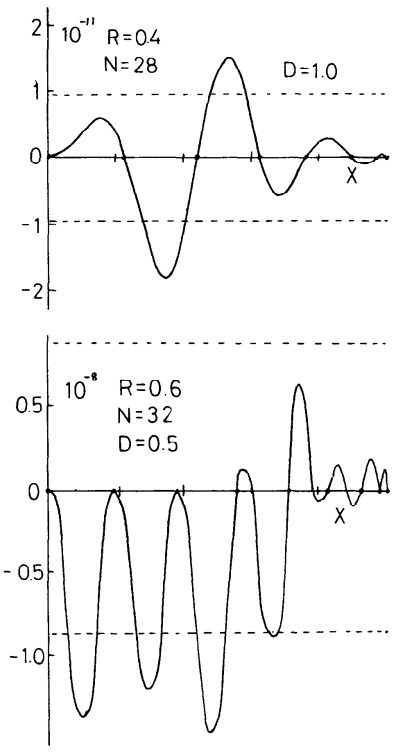

Fig. 13 Examples of error distribution on the boundary (electrode).

where M is the number of checkpoints and E_i is the error at the i-th checkpoint. In Fig. 13, we see that the maximum value of absolute error is about $1.5F$, and the absolute error is usually less than F. The horizontal axis is x, and $x=0.0$ and $x=1.0$ denote the center and tip of the electrode, respectively.

We studied the variation of error on the boundary F by charge location R and its number N. The results are shown in Figs. 14~17, where R is the abscissa, and F is the ordinate.

The error F diverges as R tends to 1 and decays logarithmically as R diminishes from 1 to 0. For very small values of R, the simultaneous equation associated with the CSM becomes unsolvable, even by a direct method, such as the Gauss Seidel method. For a value of R just before the simultaneous equation becomes unsolvable, the solution of the CSM contains many errors due to the loss of the significant digit. For such a case, the loss must be compensated for[22] by solving the simultaneous equation two or three times by a direct method. The dotted line in Figs. 14~17 denotes the limit reached by single precesion arithmetic. The upper and right area of this line can be reached. The limit for double precision is shown by dash-dot lines. There are two kinds of limit. One is the round-off error limit, and the other is when the simultaneous equation cannot be solved because of its ill-condition. At a fairly large R, if the N of the charges is large, the error F is small.

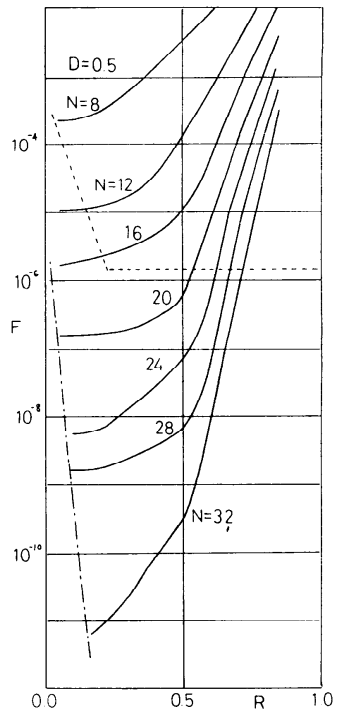

Fig. 15 Average error on the boundary (electrode of the condenser) for $D=0.5$.

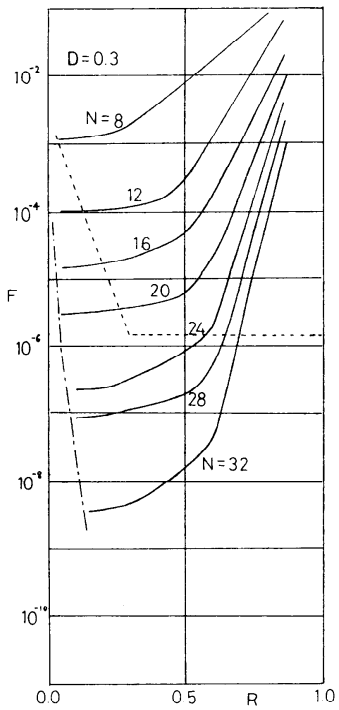

Fig. 14 Average error on the boundary (electrode of the condenser) for $D=0.3$.

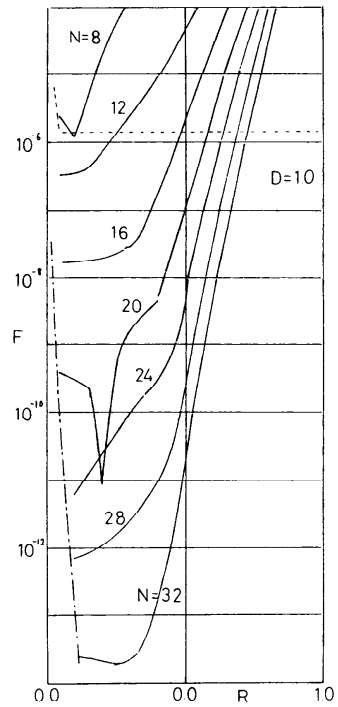

Fig. 16 Average error on the boundary (electrode of the condenser) for $D=1.0$.

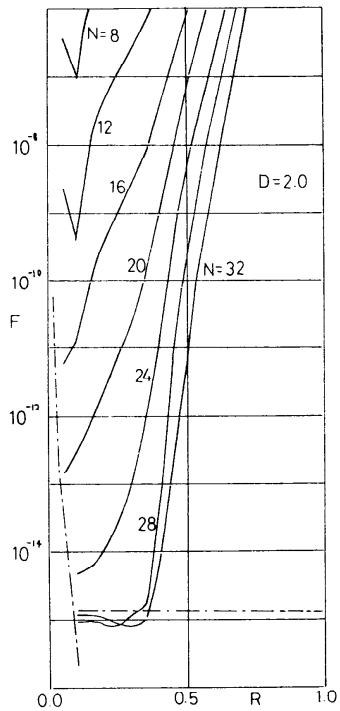

Fig. 17 Average error on the boundary (electrode of the condenser) for $D=2.0$.

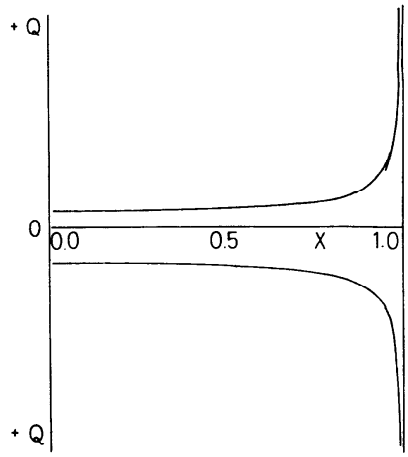

Fig. 18 Charge density on upper and lower side of electrode of higher voltage.

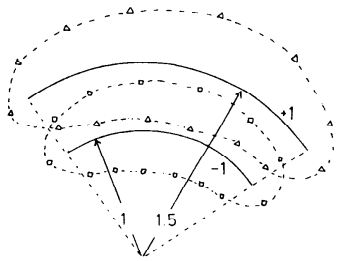

Fig. 19 Curved parallel plate condenser.

However, the error characteristics obtained by solving the simultaneous equation once by a direct method cross at a small R. This is because the degree of loss of the significant digit is large for a large N. In Figs 14~17, the loss of the significant digit is compensated for, and the inversion of the characteristics at small R disappears.

Because the error distribution curve in Fig. 13 looks different from that of the least-square approximation, greater accuracy is expected if we manipulate the contour or charge points. It is not the object of our paper to discuss how, but it is noted that our tentatively chosen charge points produce very satisfactory results with such high accuracy as we have shown in this paper. If the distance between two electrodes, D, decreases, it becomes difficult to achieve high accuracy. By simply increasing the N of the charges, a fairly high accuracy can be obtained. In Fig. 18, the charge distribution (which is proportional to the normal derivative of potential) of the upper and lower sides of the electrode is shown in arbitrary units. It seems curious that the charges on the upper and lower sides of a thin electrode distribute separately, but actually, we can obtain the charge distribution on the upper and lower sides of the electrode by computing the normal derivative of potential with indexes 1 and 2, respectively.

5.2 Curved Parallel Plate Condenser

The shape of the plate without thickness is arbitrary, which may be the straight line or a curved line. Here we consider a curved parallel plate condenser, as shown in Fig. 19. The shape of the two electrodes is a quarter of two concentric circles with radii of R1 and R2. The contour points are determined in the t-plane so that the angles viewed from the middle point of the top and bottom points of the closed line are equal (see Fig. 20 upper figure). The distances between neighbouring contour points are not equal in this way of determination. It is, however, not so different from what we hoped, because the closed line is nearly equal to an unit circle. Charge points are determined by contracting the boundary similarly to the previous problem. The number of contour points on the upper side of the closed line (shown as a bold line in Fig. 20) in the t-plane is larger than that on the lower side of the closed line (shown as a dotted line in Fig. 20). The same is true in the z-plane; that is, the number of contour points on sheet 1 is greater than that on sheet 2. The distribution of the contour points mentioned above makes the error distribution on both boundaries almost equal. If we place on sheet 1, the same number of contour points that is on sheet 2, the error on the upper side of the electrode becomes greater than that on the lower. The estimation of error F are given in Fig. 21~23 for R1=1 and R2=1.5, 3.0 and 5.0. As in the previous example, the symmetry of the right and left is not used. Hence, the number N in Fig. 21~23 can be

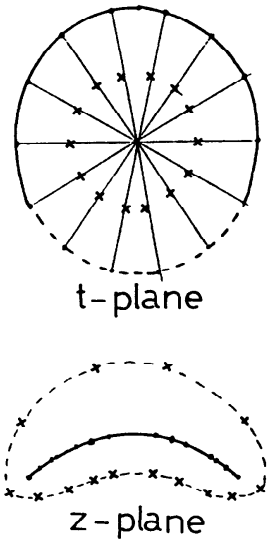

Fig. 20 Arrangement of contour points and charge points for the curved parallel condenser.

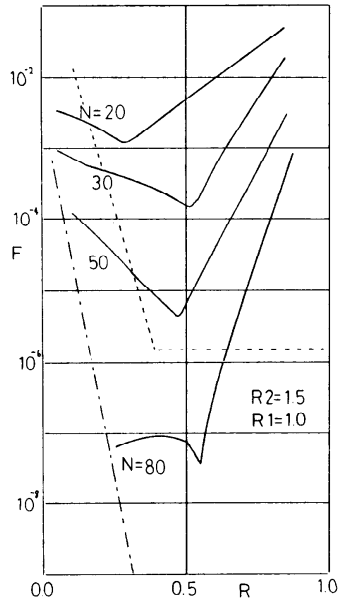

Fig. 21 Average error on an electrode of the curved condenser for $R1=1.0$ and $R2=1.5$.

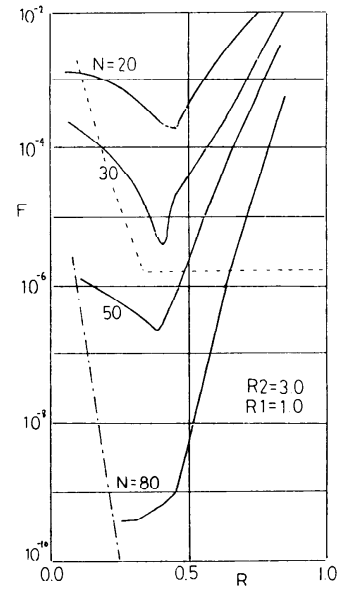

Fig. 22 Average error on an electrode of the curved condenser for $R1=1.0$ and $R2=1.5$.

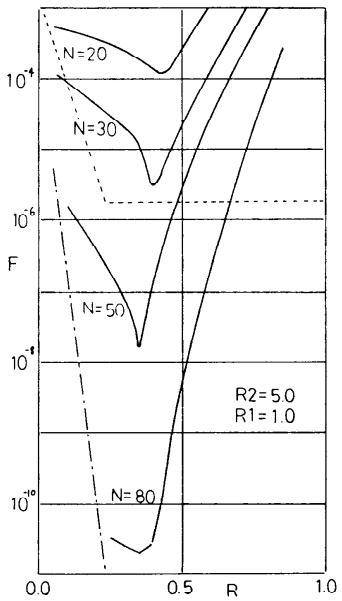

Fig. 23 Average error on an electrode of the curved condenser for $R1=1.0$ and $R2=5.0$.

halved. The relationship between the error F and the parameter R is not simple as in the previous example. As N increases, the error decreases as far as numerical experiments show, and in the range of $0.5<R<1.0$, the error decays logarithmically as R goes down. Generally speaking, we can conclude that there is an optimal value of R. Fig. 22, however, shows that the curve corresponding to $R2=3.0$ and $N=80$ decays monotonically. The increasing error, as R approaches zero, is greater than the level of loss of the significant digit, and its compensation does not suppress the error. If the distance between the electrodes tends toward zero, achieving high accuracy becomes difficult, and the solvable area of the simultaneous equation also becomes small.

6. Discussion

The boundary value problem that contains a curved arc as its boundary is difficult to solve, not only by the charge simulation method, but also by any other method. By the technique presented here, two problems in electrostatics that are known to be difficult to solve can be analyzed easily with a maximum error of 10^{-6}. Such accuracy is impossible to achieve with a discrete method such as FEM, which needs numerical interpolation to determine the value of potential at an arbitrary point. It is remarkable that the field around the tip of the curved arc is as accurate as any other point. A tip of the curved arc is transformed to a point on the smooth closed line in the t-plane. The problem in the region surrounded by such a smooth line can be analyzed with high accuracy by the ordinary CSM.

This technique must be evaluated, not only from the standpoint as the method of eliminating the singularity of the tip of the curved arc, but also from its wide applicability for solving problems in the region that contains many curved arcs of arbitrary shape as its boundary. In this paper, the general method of computing the complex function $\sqrt{z^2-1}$ with cut of arbitrary shape is presented. This fact simplies the computing procedure of this technique remarkably.

In the field of hydrodynamics, Neumann problems related to the velocity potential are common. The method known as the vortex simulation method[23] (VSM) is available for such problems. By transforming the Neumann problem concerned into a Dirichlet problem related to the flow function, one can determine the quantity of charges by the ordinary CSM. General solution in VSM is expressed by the sum of the product of the quantity of charges and the imaginary part of Green's complex function. It is troublesome that we must manage not to cross the region under consideration for the discontinuity line of the imaginary part; however we need not compute the normal derivative of the solution. The error in VSM is somewhat less than that in ordinary CSM, which treats the problem by computing the normal derivatives conventionally in Neumann type problems.[24] The VSM technique also is available for our technique of using the Riemann surface. The potential flow around the very thin plate can be analyzed effectively and accurately by combining our technique and VSM.

As an application of conformal mapping, there is a technique[18] to reduce the charge number and decrease the computing time by superposing Green's function, which satisfies a part of the boundary condition. This method also is available for our CSM using the Riemann surface.

The technique we present here is not suitable for eliminating the singularity in the problem that contains conductors with several sharp edges of non-zero angles. We think this problem must be solved by the CSM using conformal mapping, which transform the angle of a sharp edge into 180°.

The use of the CSM and our technique presented in this paper is simple in principle, is effective, and has wide applicability. For the linear Laplace equation, it is superior to a discrete method, such as the finite difference method and FEM.

Because of our fascination with sophisticated computers, we seem to have relied too much on numerical analysis, and to have abandoned the conventional analytical method. However, the appearance of the computer caused such a decisive revolution that we cannot imagine the revival of classical methods of computation. Now we must consider the most effective utilization of the computer for every kind of problem.

7. Conclusion

A new approximate method of solving the two-dimensional Laplace equation has been presented. This method is a superposition of Green's function on a Riemann surface constructed by the two-valued transformation, $z=1/2(t+1/t)$. It is suitable for analyzing potential problems in a region that contains curved arcs as its boundary. Such problems were considered unsolvable by known methods.

In the technique presented here, we regard one of two sheets of the Riemann surface as an ordinary plane on which the potential problem exists, and let the branch cut coincide with the curved arcs concerned. The poles of Green's functions are then located on the other sheet, and their influence on the first sheet is superposed similarly to the charge simulation method.

This technique is verified by analyzing test problems in electrostatics. The results are fully satisfactory. This method is applicable to the problems in a region containing many curved boundaries of arbitrary shape.

We hope that this paper will stimulate the advances of semi-analytical techniques, such as that shown here, for solving partial differential equations.

References

1. TERASAWA, K. Suugaku Gairon Oyo-hen (An Outline of Application of Mathematics), Iwanami-Shoten, Tokyo (1960).
2. KIYONO, T. Electromagnetism I, Ohmu-Sha, Tokyo (1962).
3. KAGAWA, Y. Introduction to Finite Element Method, Ohmu-Sha, Tokyo (1977).
4. TSUDA, T. Monte Carlo Method and Simulation, Baifu-kan, Tokyo (1969).
5. STEINBIGLER, H. Anfangsfeldstärken und Ausnutzungsfactoren Rotationssymmetrischer Elektrodenanordnungen, Dissertation, T. H. München (1969).
6. SINGER, H., STEINBIGLER, H. and WEISS, P. A Charge Simulation Method for the calculation of high voltage fields, IEEE, PAS-93, p 1660 (1974).
7. FINLAYSON, B. A. The Method of Weighted Residuals and Variational Principle, Academic Press, New York (1972).
8. KAWAI, T. The Method of Weighted Residuals, Lectures at Sylmposium on the Finite Element Method at Computer Center of Tokyo University (1975).
9. Technical Report of IEEJ Recent Computation of Electrical Field, to be published in 1980.
10. MASUDA, S. and MATSUMOTO, Y. Calculation of Standing

Wave by Charge Simulation Method, *Journal of IEEJ*, 93-A (1973) 305–312.
11. MASUDA, S. and KAMIMURA, T. Approximate Methods for Calculating a Non-Uniform Traveling Field, *Journal of IEEJ*, 96-A (1976) 487–494.
12. AOYAMA, M. and MASUDA, S. Theoretical Characteristics of Double-Array and Triple-Array Electric Curtain of Standing Wave Type, *Journal of IEEJ*, 95-A (1975) 505–512.
13. WEIS, P. Berechnung von Zweistoffdielektika, ETZ-A, 90, p. 683 (1969).
14. SINGER, H. Das Elektrishe Feld von Gitterelektroden, ETZ-A, 90, p. 682 (1969).
15. UTMISHI, D. Berechnung Dreidimensionaler Hochspannungsfelder, ETZ-A, 99, p. 83 (1978).
16. MURASHIMA, S., KATO, M. and MIYACHIKA, E. On the Properties of the Error in the Charge Simulation Method, *Journal of IEEJ* 98-A (1978) 39–46.
17. UNO, T. and KO, H. Potential, Baifu-kan, Tokyo (1957).
18. MURASHIMA, S. Application of Conformal Mapping to CSM, Symposium of Electrical Discharge, ED-79-3 (1979).
19. KUHARA, H. The Charge Simulation Method on Riemann Surface, Papers at Convention of IEEJ, Apr. 1979.
20. MORI, M. Numerical Analysis and Analytic Function Theory, Chikuma-Shobo, Tokyo (1975).
21. MURASHIMA, S. and KUHARA, H. Charge Simulation Method Using Green's Function on Riemann Surface, Papers at Convention of IPSJ, Jul. 1979.
22. MCCALLA, T. R. Introduction to Numerical Methods and FORTRAN Programming, John Wilwy & Sons, New York (1972).
23. MASUDA, S. and MATSUMOTO, Y. Calculation of Fluid Field by Charge Simulation Method, *Journal of IEEJ*, 96-A, (1976) 1–8.
24. KATO, M. and MURASHIMA, S. On the Application of Charge Simulation Method to Neumann Problems, Reports of Fac. of Eng. of Kagoshima University, 22 (1979) 173–180.
25. MURASHIMA, S. Application of Chagre Simulation Method to Poisson's Equation, Proceedings of the Institute of Electrostatics Japan, 4 (1980) 38–43.